Polarimetry of atmosphereless Solar System bodies

Vera Rosenbush

Main Astronomical Observatory
of National Academy of Sciences of Ukraine

Outline of presentation

- main scientific objectives
- instrumentation for observations
- polarimetry of asteroids of different types
- polarimetry of Galilean satellites of Jupiter
- polarimetry of Saturnian satellites (Enceladus, Rhea, Iapetus)
- spectropolarimetry of the major satellites of Uranus (Miranda, Ariel, Umbriel, Titania, Oberon)
- polarimetric properties of Centaurs and TNOs according to published data
- mechanisms of light scattering and their predictions
- stratification of the polarization properties of small bodies in the Solar System

Particle characterization

Regolith surfaces

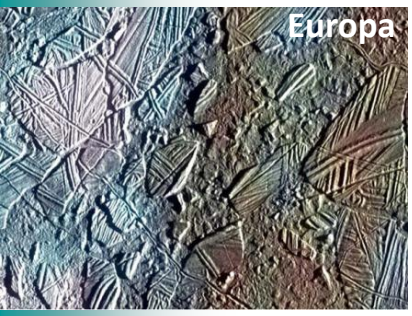

Diversity of surfaces and particles

Atmosphereless bodies are covered by a porous, optically thick dust or icy layer of interacting particles, called the regolith.

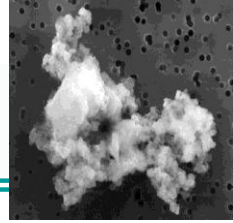

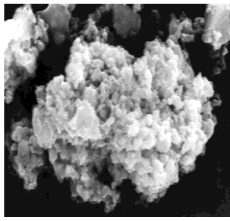

IDPs
(cometary particles)

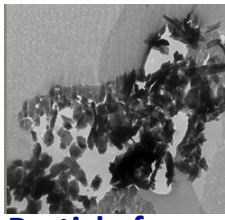

Particle from
comet Wild 2

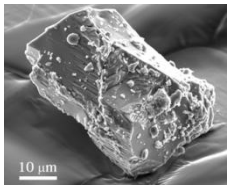

Particle from
asteroid Itokawa

Scientific objectives:

1) Determination of the physical properties of surfaces as well as single dust particles in different small bodies.
2) Study of light scattering mechanisms.
3) Better understanding of the origin and evolution of Solar System bodies.

Io

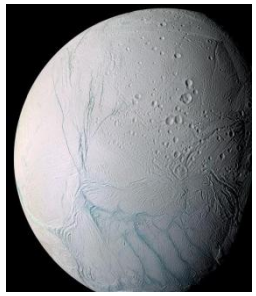

Enceladus

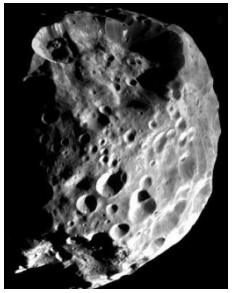

Phoebe

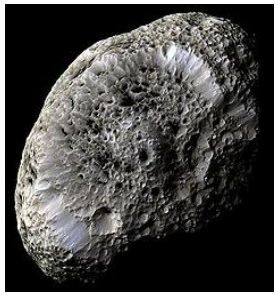

Hyperion

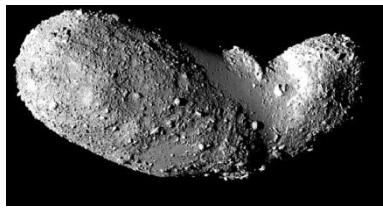

Asteroid Itokawa

Telescopes, polarimeters, filters

Telescopes of CrAO, Ukraine

AZT-11, 1.25 m

ZTSh, 2.6 m and aperture polarimeter

SAO RAS, Russia

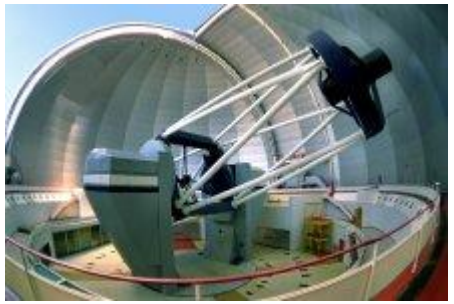

6-m telescope

Polarimetry of asteroids, Jupiter and Saturn moons

Instrumentation: aperture photopolarimeters

Telescopes: 2.6 m (CrAO, Ukraine)
1.25 m (CrAO, Ukraine)
0.7 m (Grakovo, Ukraine)

Filters: standard UBVRI bands and the broadband red filter WR (690 – 930 nm)

Two single-channel aperture photopolarimeters with rapidly rotating polarizers (~33 rotations per second) are mounted at the 2.6-m and 0.7-m telescopes *(Mishchenko et al. 2010 for details).*

The UBVRI photopolarimeter are mounted at the 1.25-m CrAO telescope *(Piirola 1988; Berdyugin& Shakhovskoy 1993).*

Spectropolarimetry of the major moons of Uranus and comets

Instrumentation: SCORPIO-2 focal reducer

Telescope: 6-m (SAO, Russia)

Phase-angle curves of brightness and polarization

Brightness opposition effect and negative linear polarization

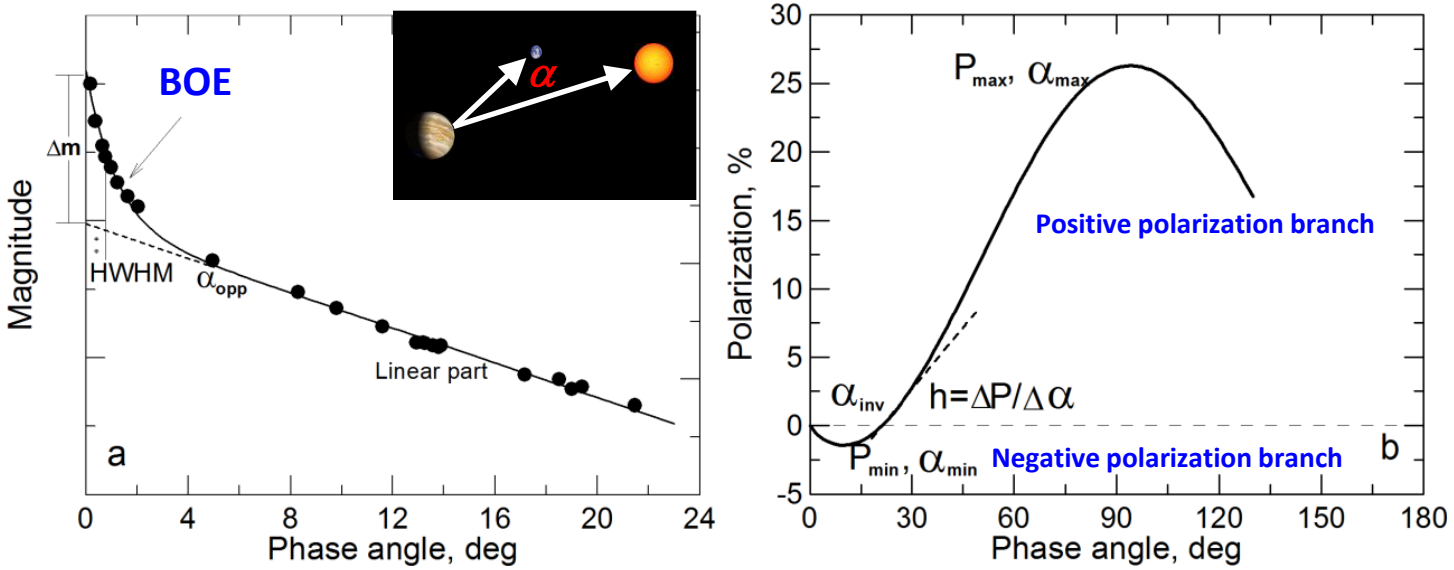

Typical phase-angle dependences of brightness and polarization

The phase curves of brightness and polarization and their spectral dependences are controlled by the light scattering mechanisms and are related to the physical properties of the scattering media such as the size, morphology, composition, and packing of the constituent particles.

Negative linear polarization means that the electric field vector component parallel to the scattering plane dominates the perpendicular component.

Polarimetry of asteroids

Composite phase curves of polarization for C-, S-, and E-type asteroids

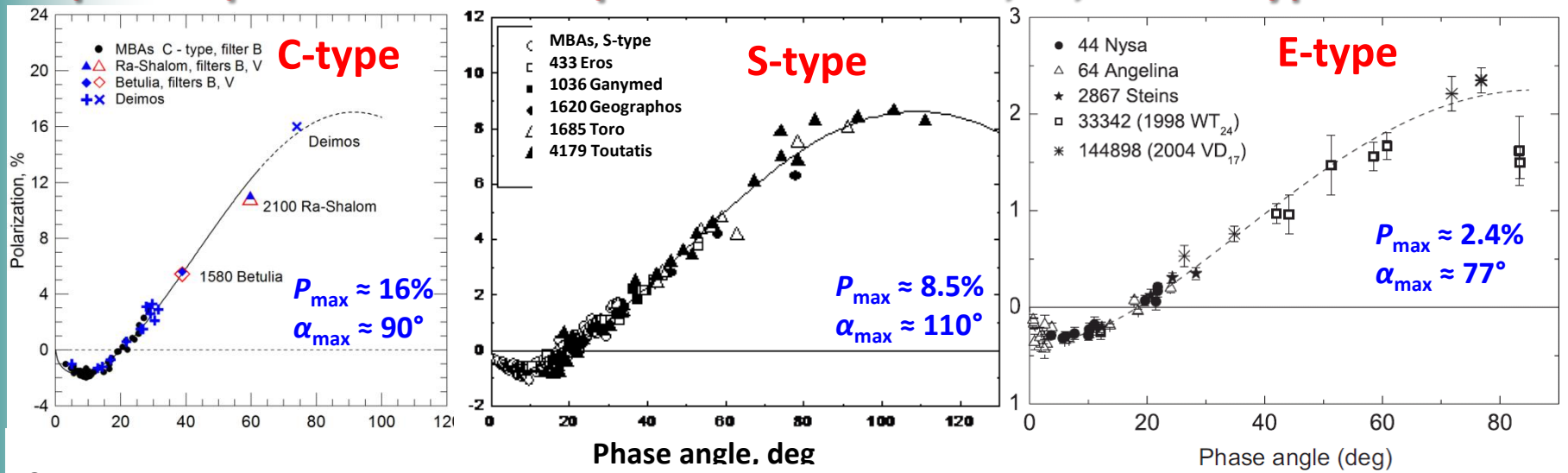

C-type *(Kiselev et al. 1999;* Zellner 1972; Noland et al. 1973; Tedesco et al., 1978*);*
S-type *(Kiselev et.al.1990, 1994; Lupishko et al. 1995; Belskaya et al. 2009);*
E-type (*Kiselev et al. 2002;* Fornasier et al. 2006; De Luise et al. 2007).

From polarimetry and photometry we can obtain:

- parameters of phase-angle dependence of polarization;
- classification of asteroids into types;
- albedo and diameter of asteroids
- size of particles
- composition and structure of regolith surface

NEA 33342 (1998 WT_{24}):
E-type, p_v= 0.43,
size 0.42 x 0.33 km,
particles size 18–30 µm
(Kiselev et al. 2002)

Future task: Determinate the parameters of phase curve of polarization for other types of asteroids.

Negative polarization branch for asteroids

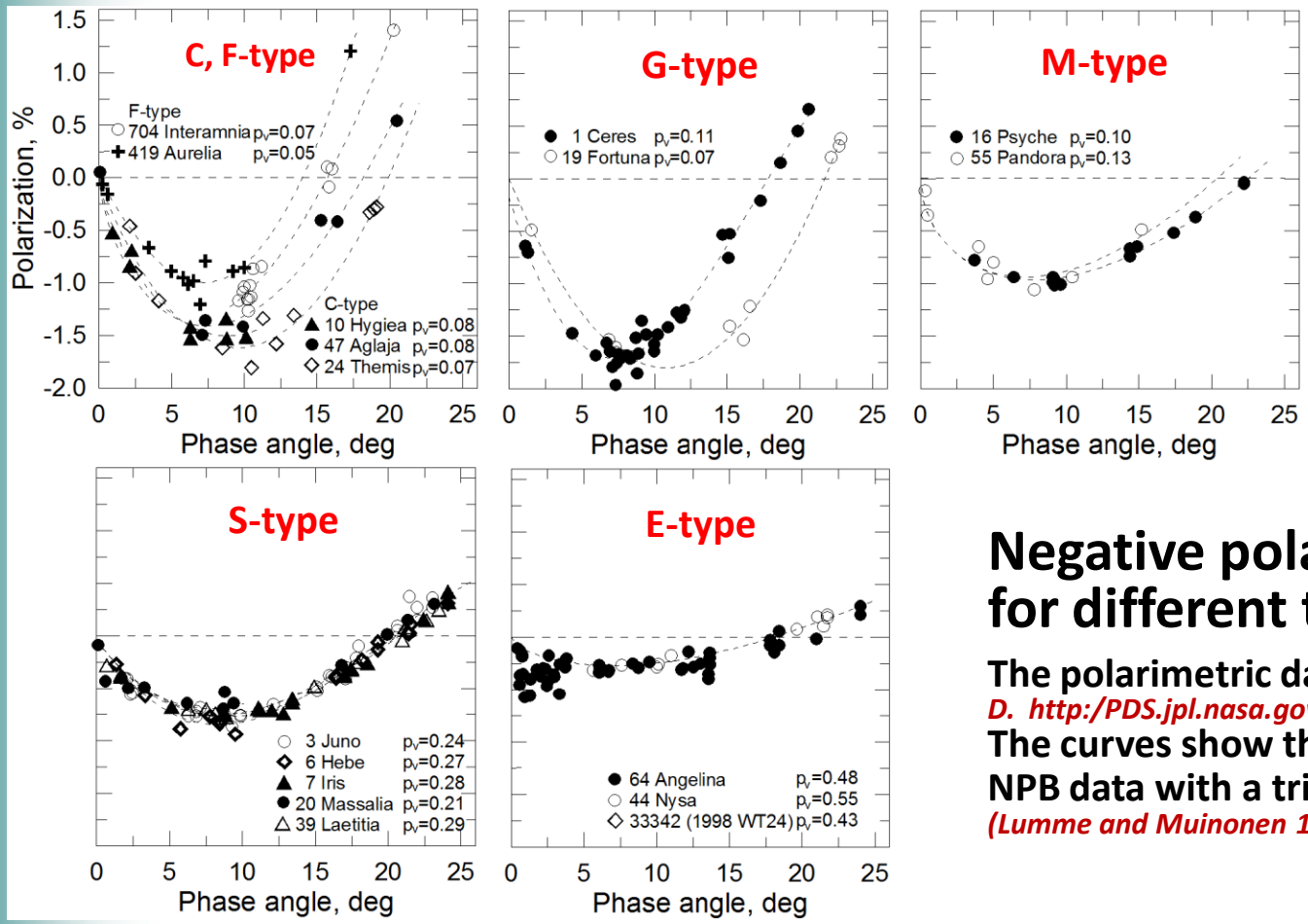

Negative polarization branch for different types of asteroids.

The polarimetric data are taken from *(Lupishko D. http:/PDS.jpl.nasa.gov (APD; Rosenbush et al. 2005)).*
The curves show the approximation of the NPB data with a trigonometric polynomial *(Lumme and Muinonen 1993; Penttilä A. et al. 2005).*

- there is a great variety of phase curves for low-albedo asteroids and it is impossible to describe data by a unique curve;
- the data for moderate and high-albedo asteroids are more uniform.

Asteroids with anomalous polarization

According to published data *by Cellino, Gil-Hutton, Belskaya, et al.*

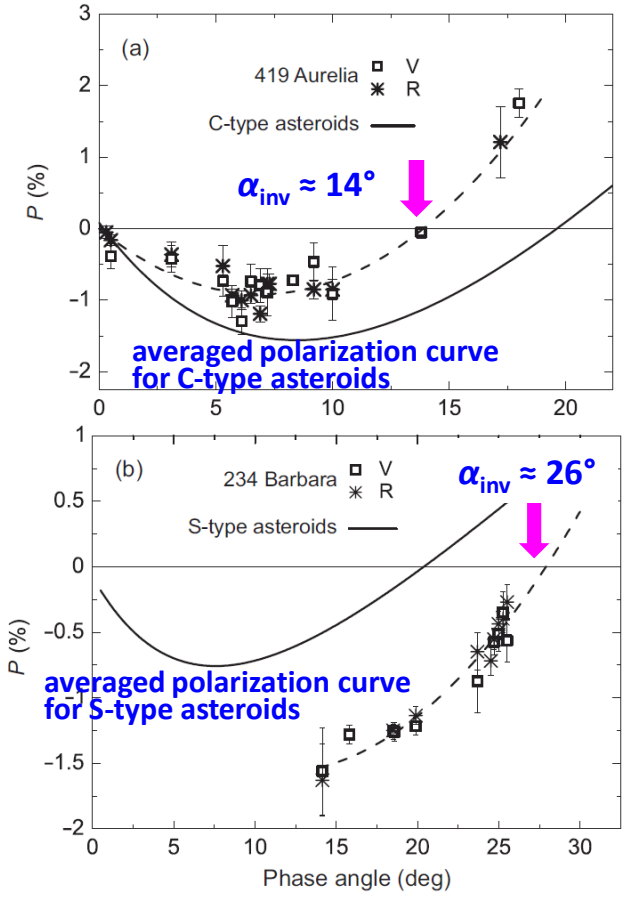

Polarization phase dependences for asteroids 419 Aurelia (a) and 234 Barbara (b) according to *(Belskaya et al. 2005; Cellino et al. 2006, 2007).*

Several F-type asteroids have anomalous polarimetric properties with shallow NPBs and small inversion angles.

Several S-type asteroids have wide NPBs with large inversion angles similar to that measured for Barbara *(Gil-Hutton et al. 2008; Masiero and Cellino 2009).*

The anomalous polarimetric properties of these asteroids could be related to a specific structure of regolith surface and composition, which are considered to be the most primitive composition preserved from the early stages of the evolution of the Solar System *(Belskaya et al. 2005)*

Polarization opposition effect

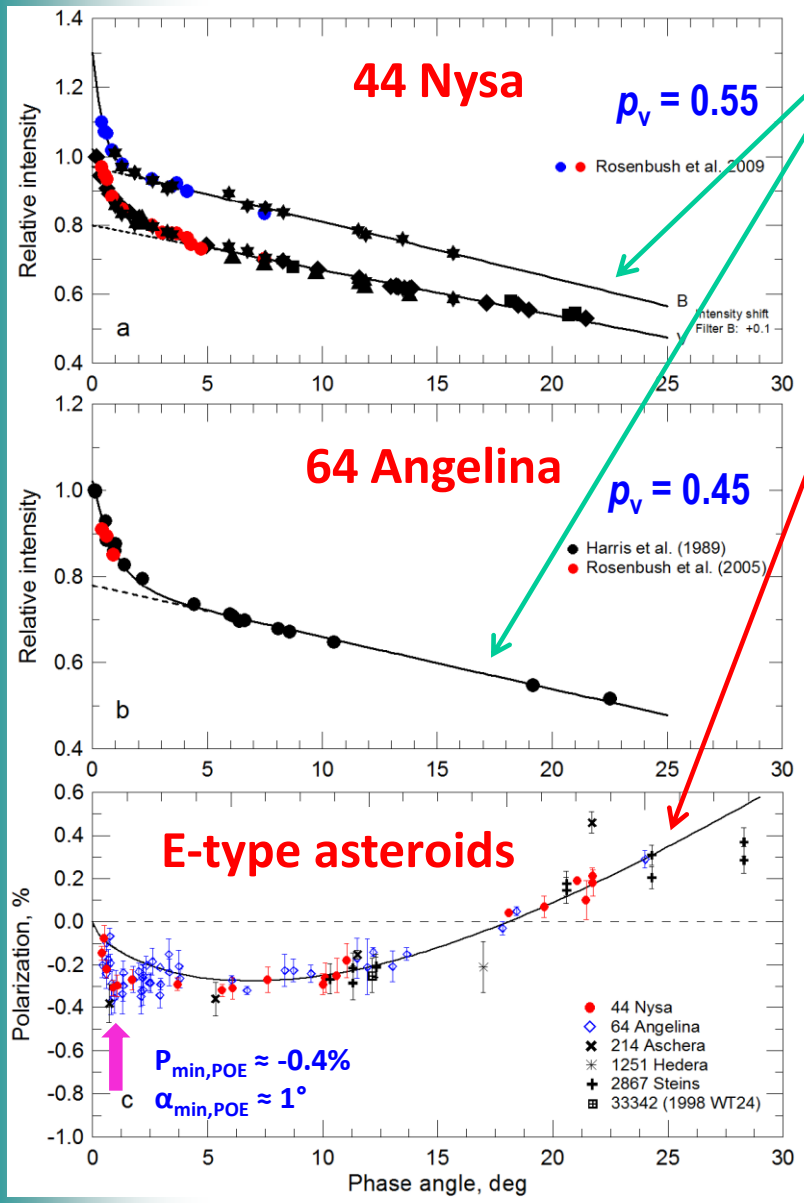

Composite phase curves of brightness for asteroids 44 Nysa (a) and 64 Angelina (b).

Photometric data were obtained in the 1979, 1982, 1986, 1987, and 2005 apparitions *(Birch et al. 1983; Tupieva 2003; Shevchenko et al. 1992; Harris et al. 1989; Rosenbush et al. 2005, 2009)*

Composite phase curve of polarization for E-type asteroids based on all available data in the V and R filters for different oppositions

(Zellner and Gradie 1976; Kiselev et al. 2002; Belskaya et al. 2003; Rosenbush et al. 2005, 2009; Fornasier et al. 2006a, b; data by Kiselev & Lupishko from APD; Cellino, personal communication).

Polarization measurements for Nysa and Angelina were obtained in the 1995, 1999, 2000/01, 2008, 2009, 2011 apparitions *(Rosenbush et al. 2005, 2009; unpublished data by Kiselev, Rosenbush, Zaitsev)*.

There is a sharp minimum of negative polarization centered at α_{min}≈1° and having amplitude about 0.4%. This opposition phenomenon is called by the polarization opposition effect.

The phase angle of polarization minimum corresponds to the semi-width of brightness opposition effect.

S-, V-, and F-type asteroids

4 Vesta, 20 Massalia, 419 Aurelia, 1021 Flamario

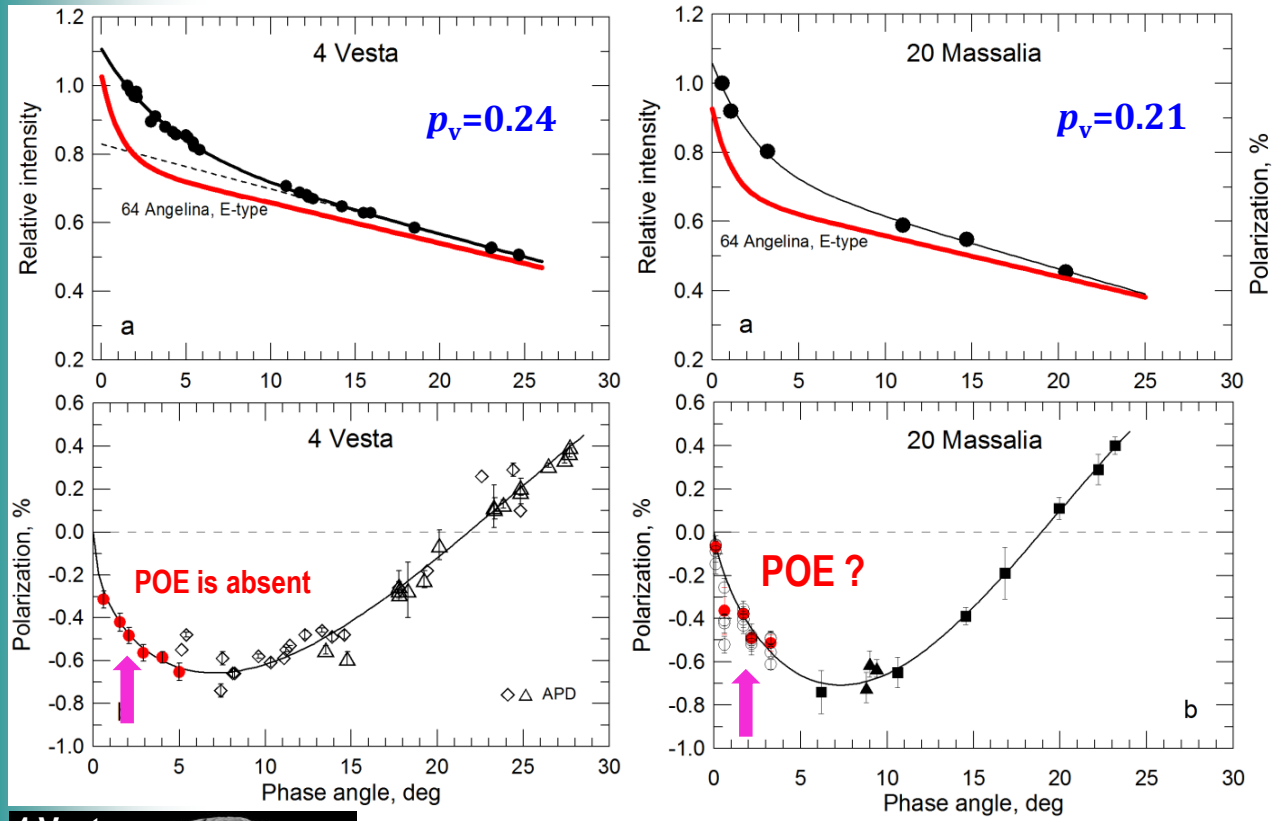

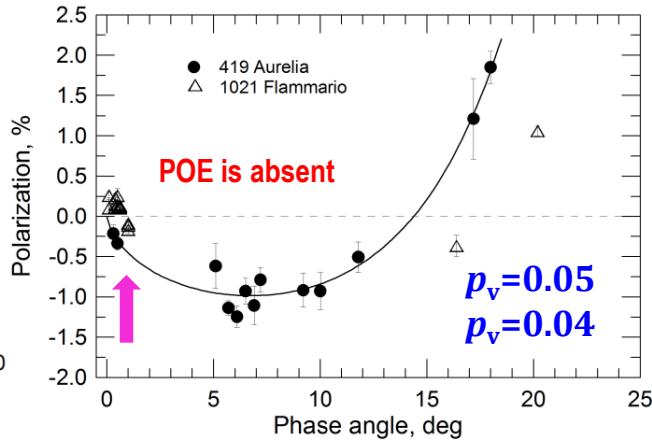

Degree of polarization for low-albedo F-type asteroids 419 Aurelia and 1021 Flammario as measured by *(Belskaya et al. 2005; Fornasier et al. 2006).*

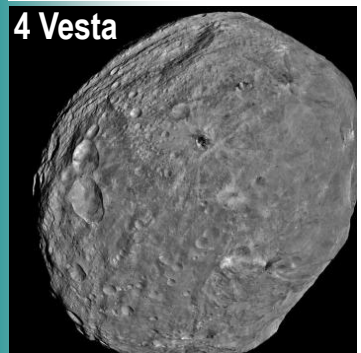

Phase-angle dependence of brightness (a) and polarization (b) for asteroids 4 Vesta and 20 Massalia.

For comparison, the phase curve of brightness for E-type asteroid 64 Angelina are shown *(Rosenbush et al. 2002, 2006; APD).*

The POE is absent for moderate- and low-albedo asteroids

Opposition effects for Jupiter satellites

Io

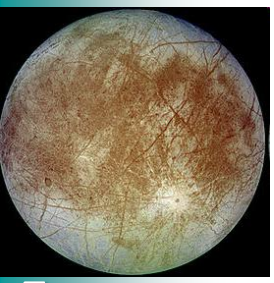

Europa

Ganymede

Europa, p_V=0.68;

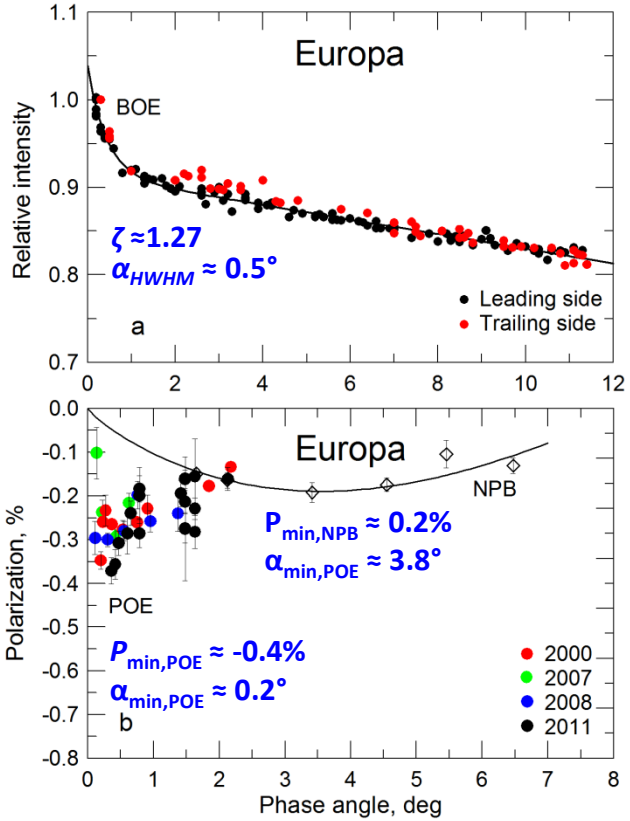

The brightness *(Thompson&Lockwood 1992)* (a) and polarization *(Rosenbush & Kiselev 2005)* (b) opposition effects for Europa in the V band.

Io, p_V=0.62; Ganymede, p_V=0.44

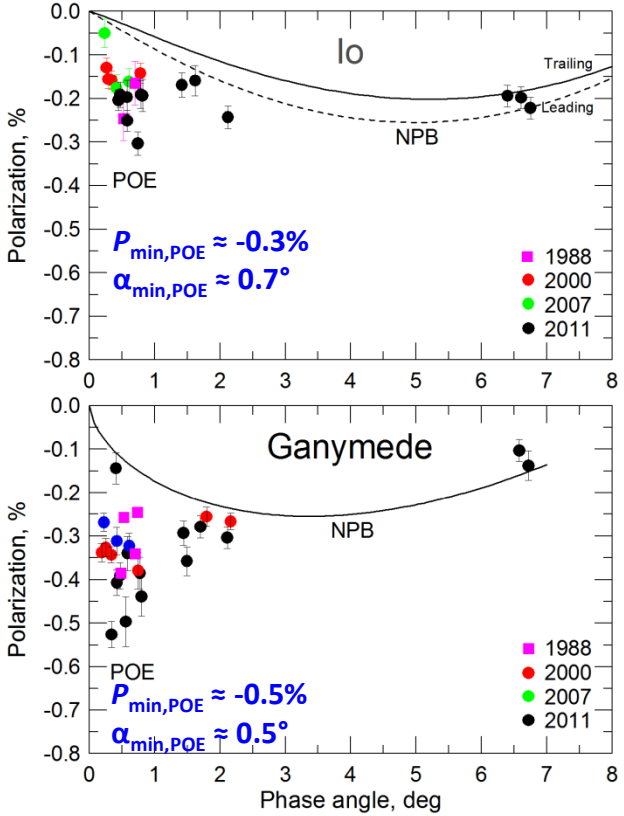

The polarization opposition effects for Io and Ganymede in the V band *(Rosenbush & Kiselev 2005).*

A bimodal phase-angle dependence of polarization is found for high-albedo Galilean moons. One branch is a narrow asymmetric peak of negative polarization with the minimum at 0.2 – 0.7°. Another branch is a regular phase-angle curve of polarization.

Opposition effect for Jupiter satellites

Callisto, p_v=0.20

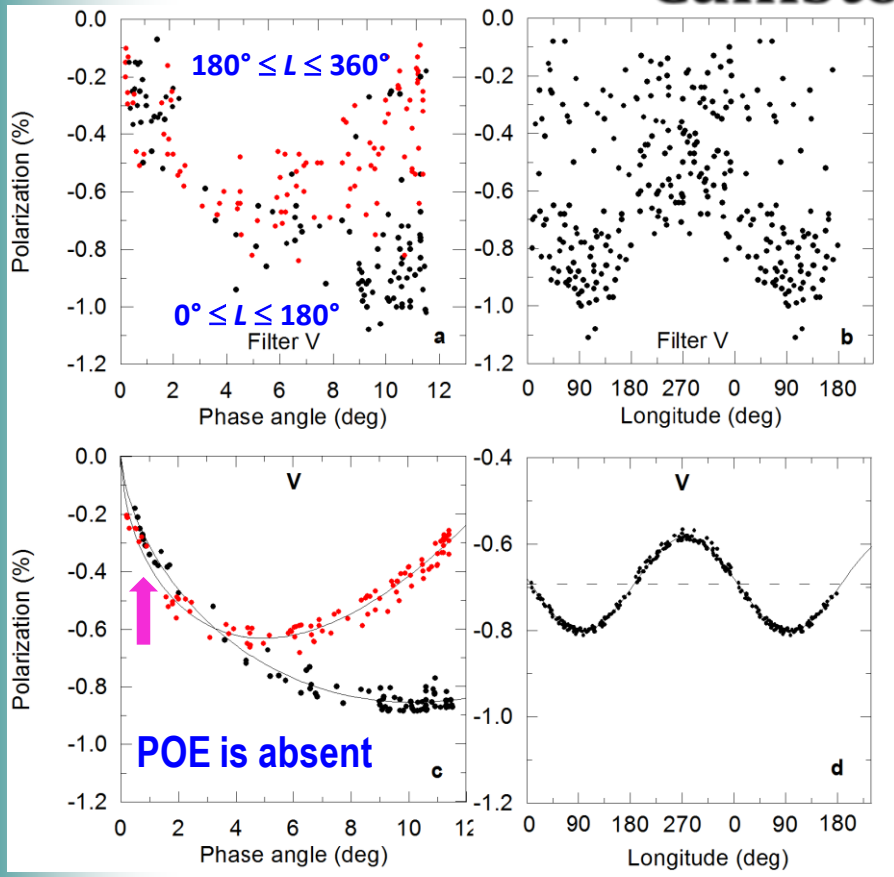

(a) Degree of polarization *vs* phase angle.

red circles – polarization for the trailing side;
black circles – polarization for the leading side.

(b) Degree of polarization *vs* longitude.

The scatter might be attributed to the local inhomogeneity of the satellite surface, which is superimposed on the global distinctions of polarimetric properties of the leading and trailing hemispheres.

$P(\alpha,L) = P1(\alpha) + P2(L,\alpha)$ - method of successive iterations

(c) Phase dependenses of polarization for the leading (black circles) and trailing (red circles) hemispheres of Callisto after taken into account the variations of polarization with orbital longitude.

(d) Longitude dependence of polarization for Callisto at phase angle $\alpha = 6°$ after taken into account the phase-angle dependence of polarization *(Rosenbush 2002).*

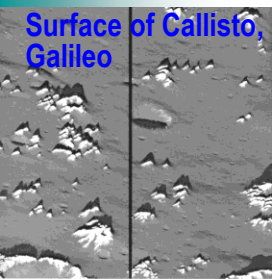

The polarization opposition effect is absent for Callisto

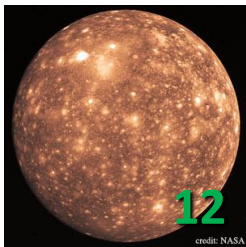

Opposition effect for Saturn moons

Iapetus: leading side, p_v≈0.04; trailing side, p_v≈0.5

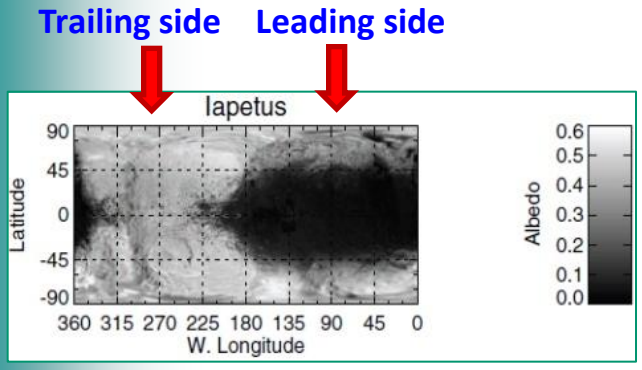

Albedo distribution on Iapetus derived from a mosaic of Cassini images

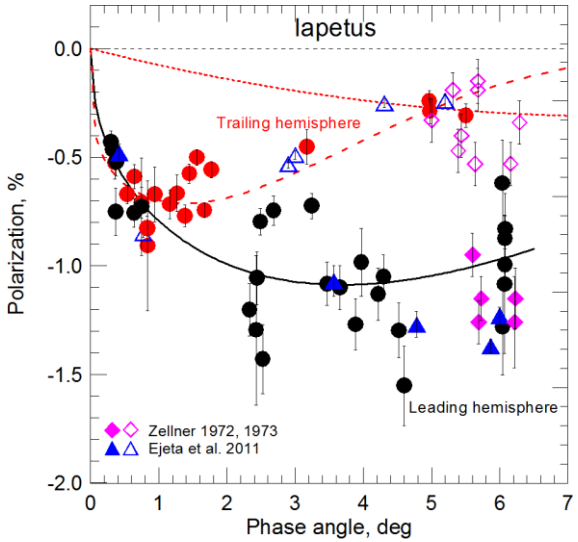

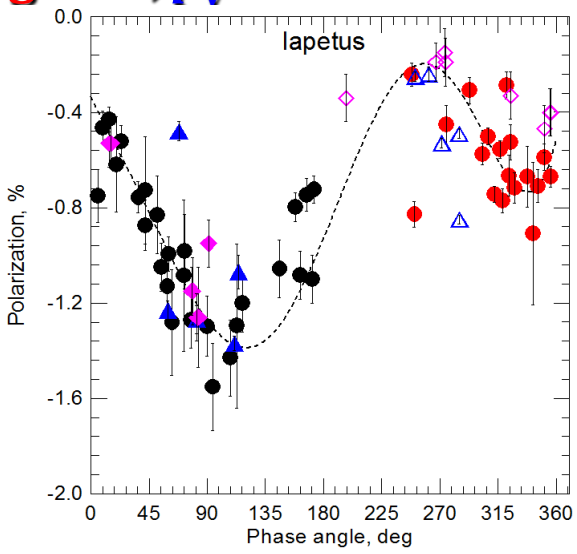

Polarization degree *vs* phase angle (a) and polarization degree *vs* longitude (b) for Iapetus obtained during the 1998 – 2012 period.

The respective NPB are shown schematically for the leading (filled symbols) and trailing (open symbols) hemispheres. Diamonds and triangles show the polarization data taken from *(Zellner 1972, 1973)* and *(Ejeta et al. 2011)* respectively.

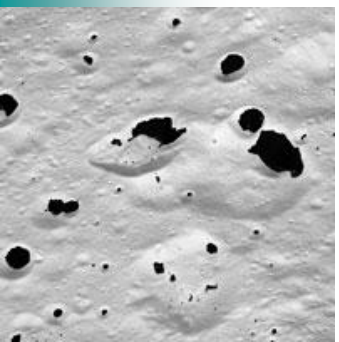

There is no a secondary minimum near opposition for the dark leading hemisphere of Iapetus.

The bright-side polarization of Iapetus measured at Δα= 4°–6.4° is a typical value for the regular NPB for high-albedo objects at the corresponding phase angles.

A strongly asymmetric phase curve of polarization with minimum at α ≈ 1.5° cannot be excluded.

Opposition effects for Saturn moons

Enceladus, p_v=0.99; Rhea, Dione, p_v=0.7

Enceladus has the highest albedo of any object in the Solar System, reflecting nearly 100% of the sunlight it receives.

Rhea and Diona are very similar in composition and albedos. Rhea is one of the most heavily cratered satellites in the Solar System.

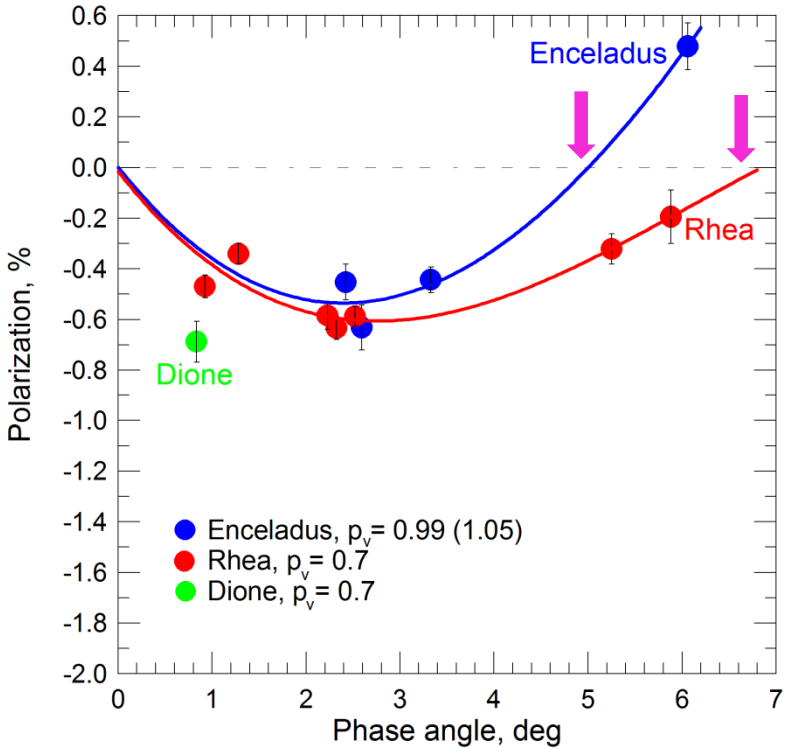

Phase-angle dependence of polarization for Enceladus , Rhea, and Dione

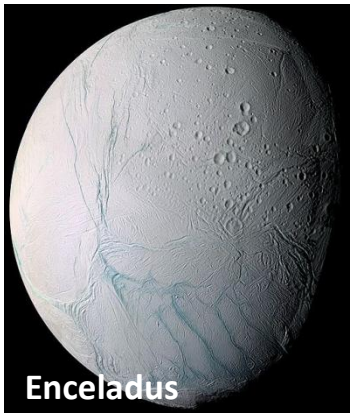

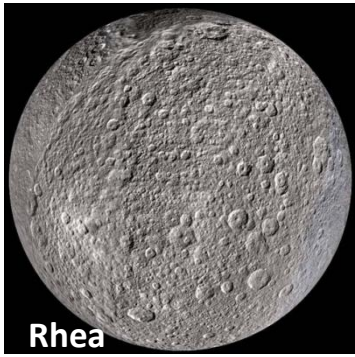

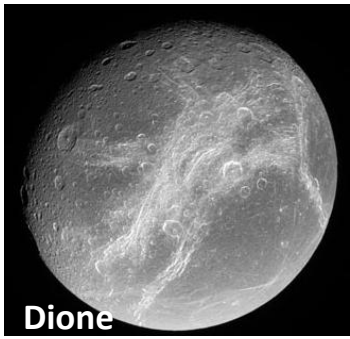

(taken by Cassini)

Enceladus has the inversion point at the smallest phase angle as compared to any other ASSB observed so far, $\alpha_{inv} < 5°$. Minimum of polarization for these satellites is at 2° ÷ 3°.

14

Opposition effects for Saturn rings

Maxwell 1856; Salo et al. 2010

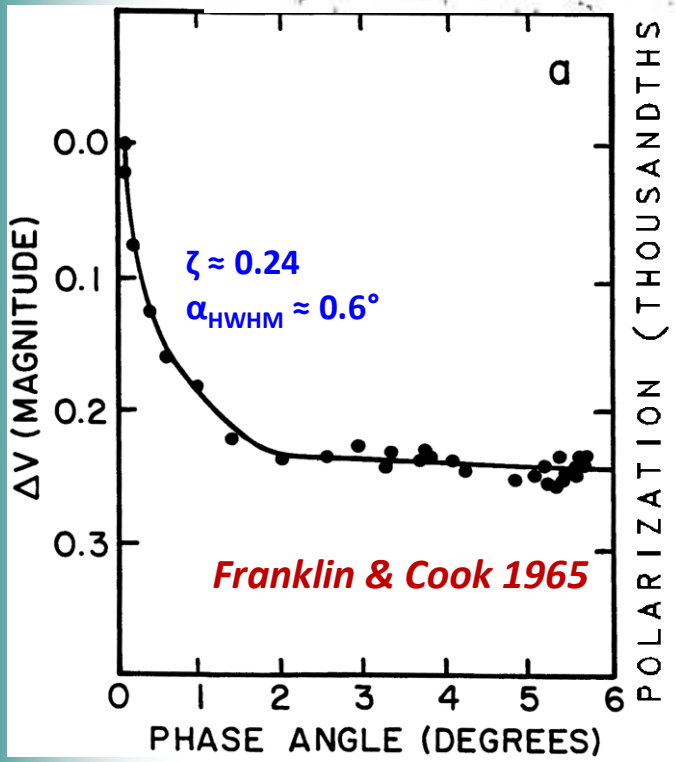

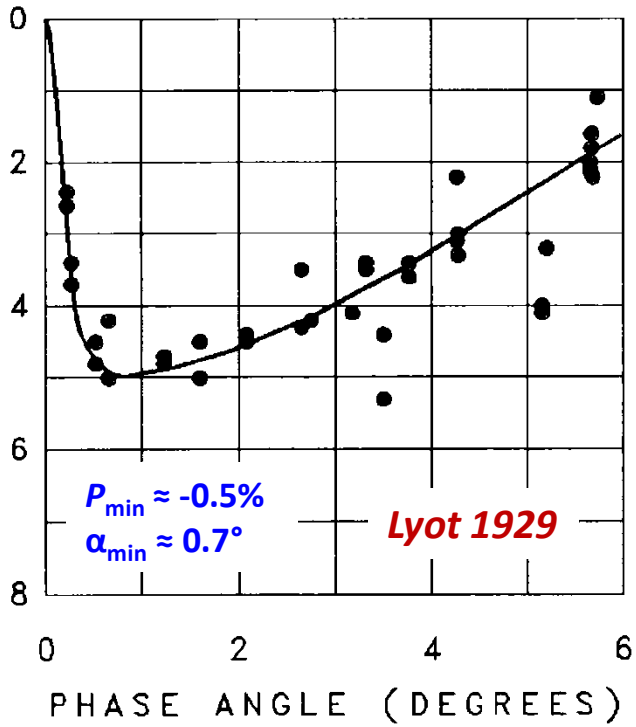

According to Lyot, NPB has a very asymmetric shape with $\alpha_{min} \approx 0.7°$, that is close to the semi-width of BOE.

Phase-angle dependences of brightness and polarization for the A and B Rings of Saturn.

Opposition effects for Uranus moons

Miranda, Ariel, Umbriel, Titania, Oberon

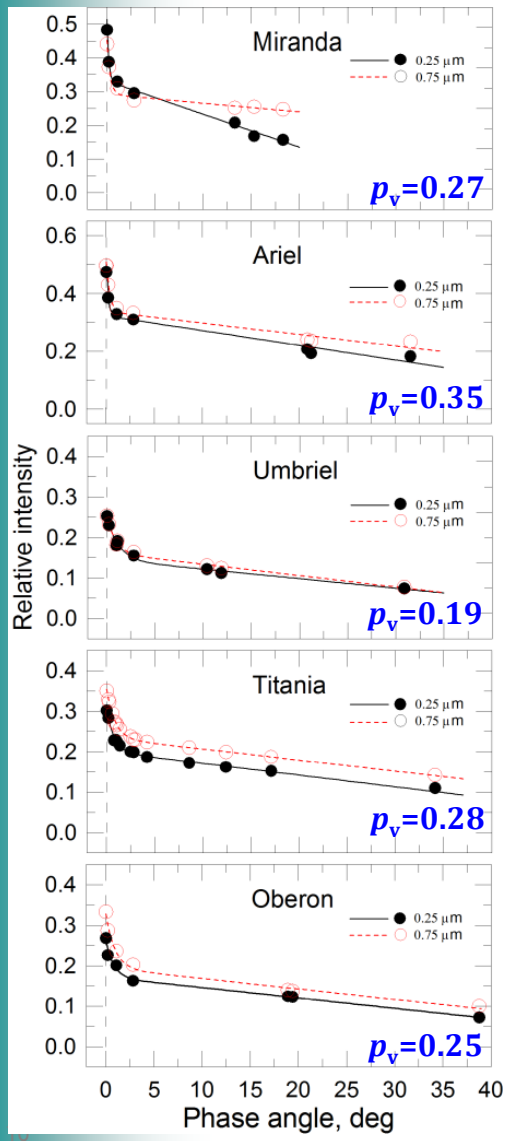

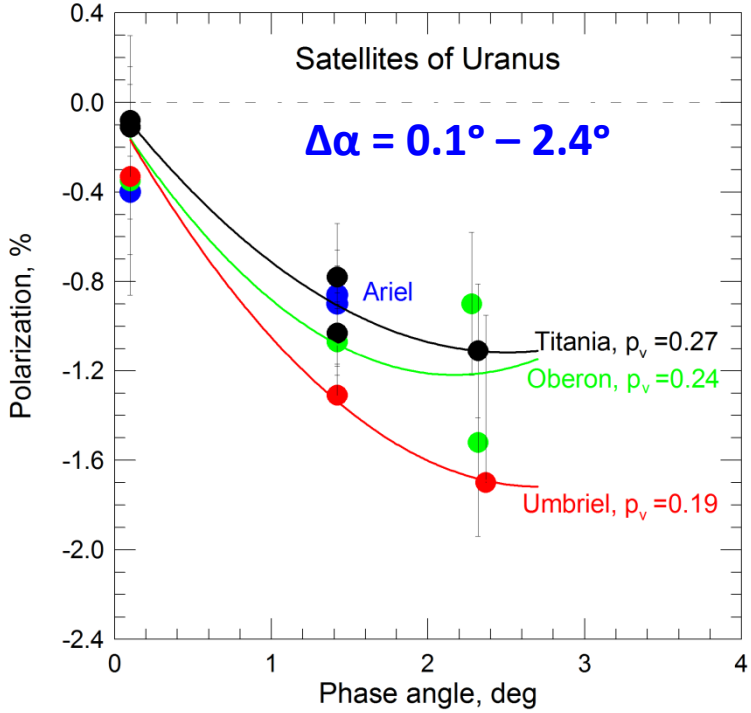

Phase-angle dependence of brightness *(Avramchuk et al. 2007)* and polarization for major satellites of Uranus

Polarization minima are shifted toward the smallest phase angles as compared to other ASSBs observed so far. The degree of polarization for the dark Umbriel at phase angle 1° is about -1.2%, while for brighter Ariel is -0.8%.

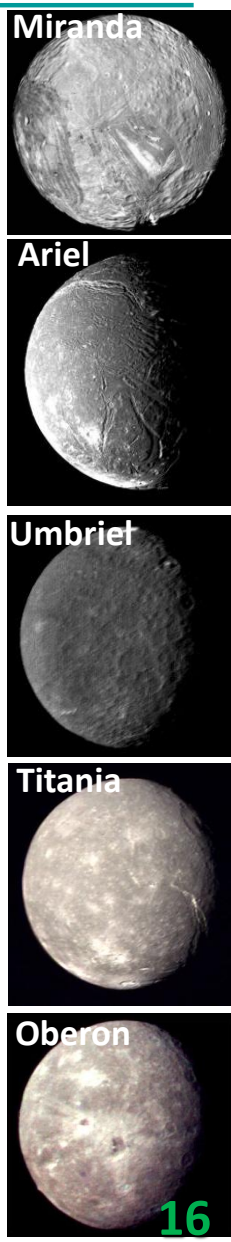

Polarimetry of Centaurs and TNOs

According to *Boehnhardt et al. (2004), Rousselot et al. (2005), Bagnulo et al. (2006, 2008),* and *Belskaya et al. (2010),* the following observational results are obtained (see Fig.):

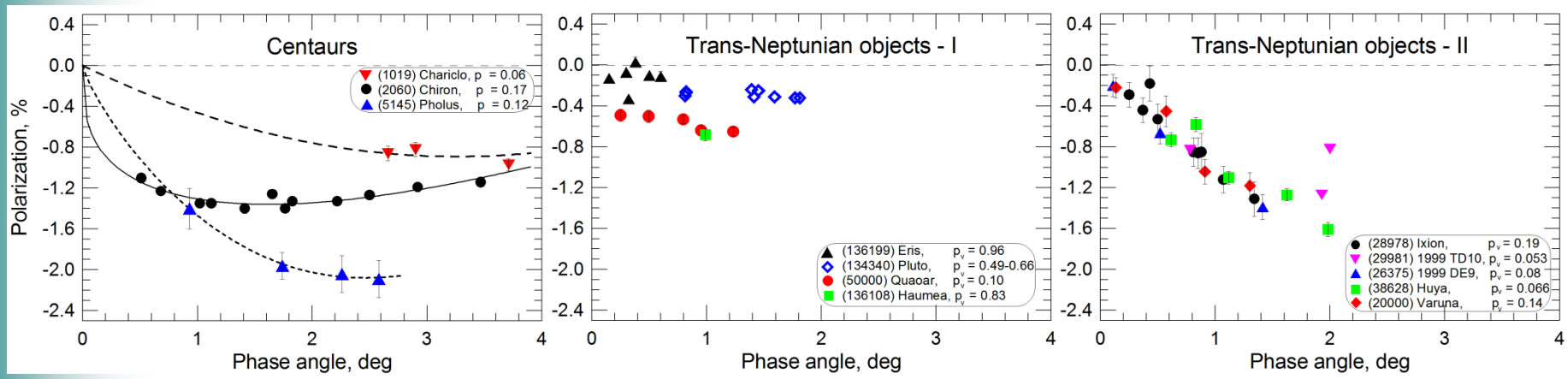

- **Centaurs exhibit different $P(\alpha)$ with P_{min} varying from −0.8% to −2.2% at $\alpha \approx 2.5° – 3.8°$;**
- **there are two classes of TNOs with different polarimetric behavior:**
  - **(i) large TNOs (D>1000 km) show relatively weak and nearly constant polarization in the observed phase range;**
  - **(ii) smaller TNOs (D<750 km) exhibit rapid increase *P* with phase angle, reaching $P \approx -1.2\%$ at $\alpha = 1°$**

17

Polarization properties of ASSBs

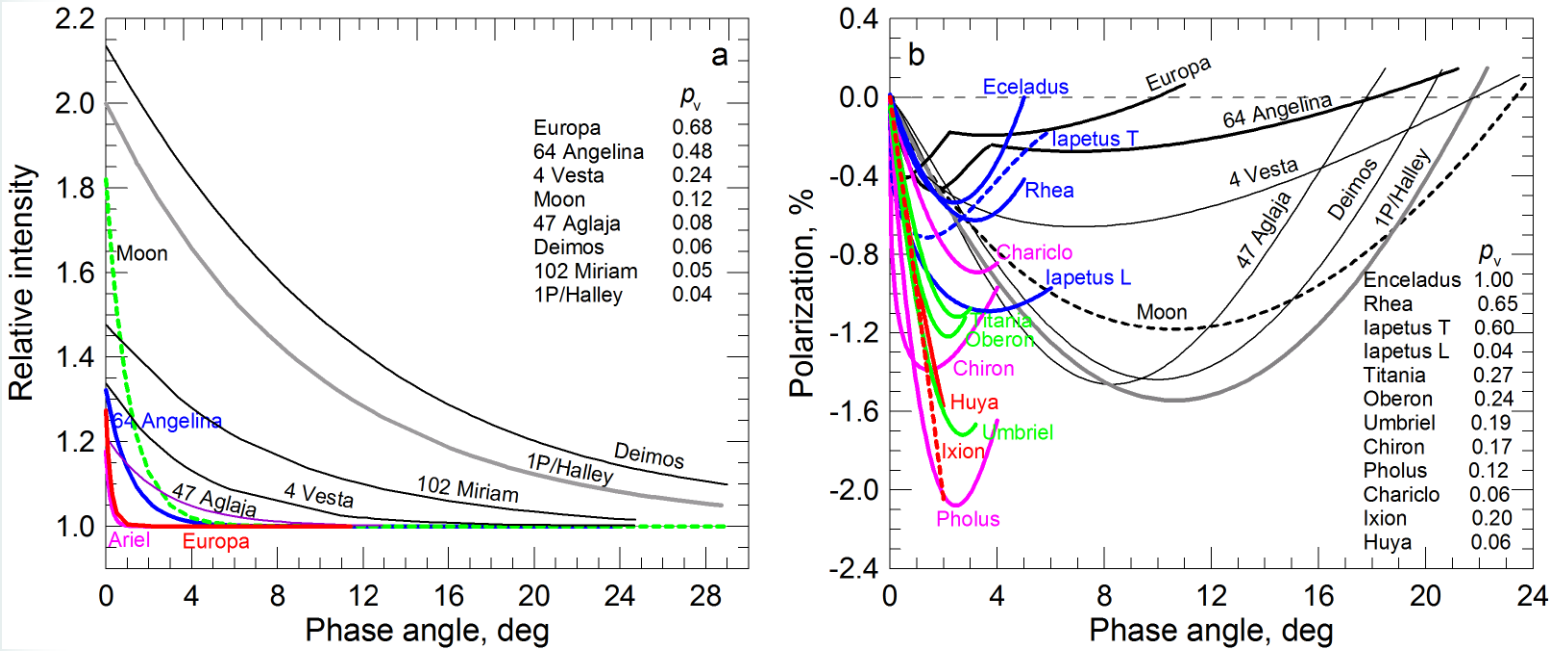

Comparison of the phase curves of brightness after subtraction of the linear part (a) and polarization phase curves (b) for different objects.

POEs are shown for satellite Europa and asteroid 64 Angelina. Blue curves – moons of Saturn; green curves – moons of Uranus; rose curves – Centaurs, red curves – TNOs.

The negative polarization branches for objects belonging to the inner part of the Solar System differ considerably from those for objects residing in the outer part.

It appears that the observed polarization of objects from the inner part is generally related to their albedos, whereas the polarization observed for distant objects cannot be explained solely by the brightness of the surface material.

Polarization *vs* distance from the Sun

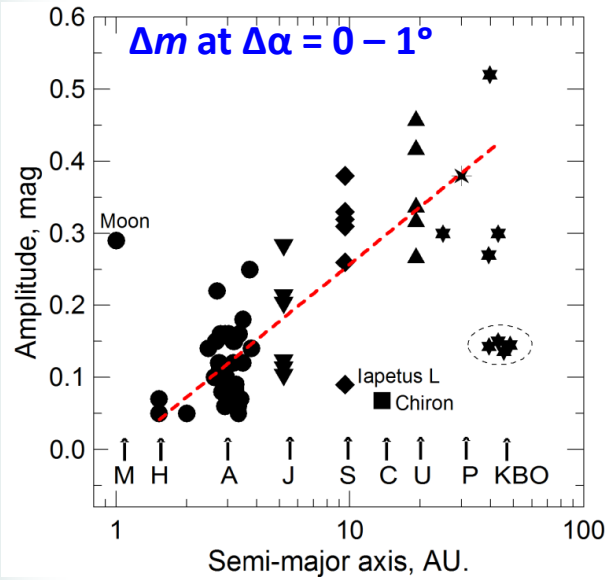

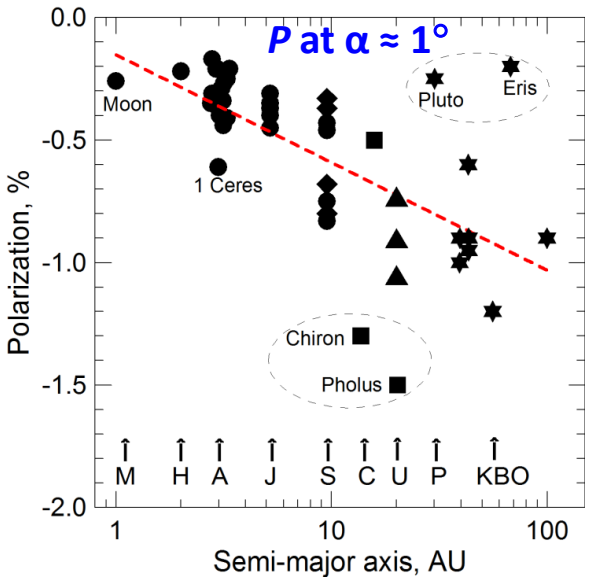

Designations:
M – Moon;
H – comet 1P/Halley;
A – asteroids;
J – Jupiter satellites;
S – Saturn satellites and rings;
C – Centaurs;
U – Uranus satellites;
P – Pluto;
KBO – Kuiper Belt objects.

Variations of amplitude of brightness and the value of polarization for different objects are shown with the distance from the Sun.

Large-amplitude BOEs and unusually strong polarization for distant objects may be indicative of a specific composition and/or microstructure of their surfaces. These properties may be caused by a relatively weak insolation of primitive materials typical of the outer regions of the Solar System. An example would be irradiated ices enriched by organic matter.

Thus, the composition and structure of the surfaces of small bodies should vary with their distance from the Sun rather than being determined solely by the objects evolution.

Light scattering mechanisms

Main factors controlling the observed opposition effects

(Mishchenko, Rosenbush, Kiselev, et al. 2010 and references therein):

- coherent backscattering (CB);
- shadowing hiding (SH);
- near-field effects (NFE);
- first-order scattering (FOS) by individual particles.

The relative contributions of these factors depend on the physical parameters (refractive index, packing density, particle morphology, and size distribution, etc.) of the regolith layer and the scattering geometry.

Theoretical predictions

- Being the result of multiple scattering, CB is to be observed for high-albedo ASSBs rather than for low-albedo objects.
- The phase-angle dependence of polarization for low-albedo objects is primarily controlled by the single scattering and near-field effects, including mutual particle–particle shielding and shadowing hiding *(Tishkovets 2008)*.
- CB causes the BOE as a narrow intensity peak centered at exactly the opposition.
- BOE must be accompanied by the POE provided that the regolith grains have sizes comparable to or smaller than the wavelength *(Mishchenko 1993; Mishchenko et al. 2000, 2009)*.
- The angular width of the POE must be comparable to that of the BOE.
- NFEs tend to decrease the intensity of backscattered light and contribute to NPB.
- Single scattering by individual particles can also contribute to the BOE and NPB.

A comparison of observational results and theory show that there is a class of high-albedo ASSBs with unique opposition properties which are in a reasonable quantitative agreement with the existing theory *(Mishchenko et al. 2006, 2009, 2010)*.

Light scattering theory

Current numerical capability: polydisperse particles

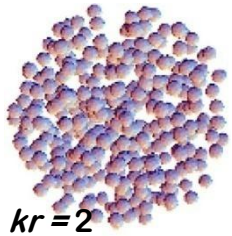

Direct, numerically exact solution of the Maxwell equations

$kR = 40$, $m_1 = 1.31$, $m_2 = 1.5$, $kr_1 = kr_2 = 4$

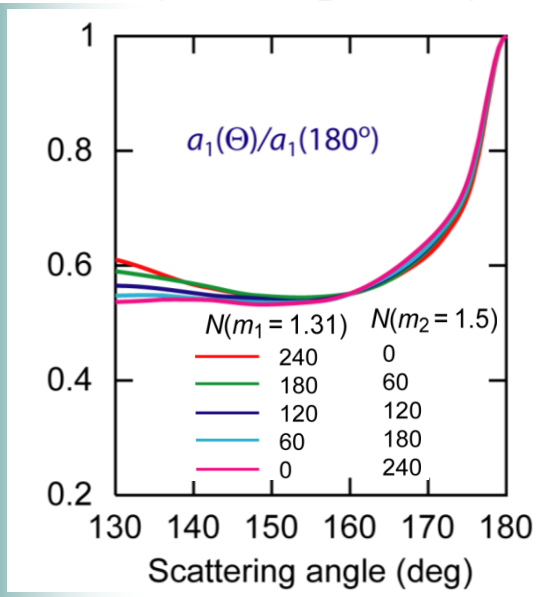

Mackowski & Mishchenko 2011

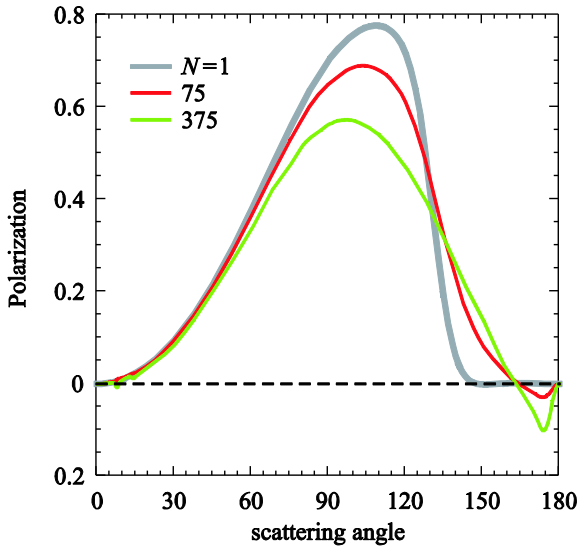

$N = 375$, $\rho = 0.1$
$m = 1.31$, $kR = 31$, $kr = 2$

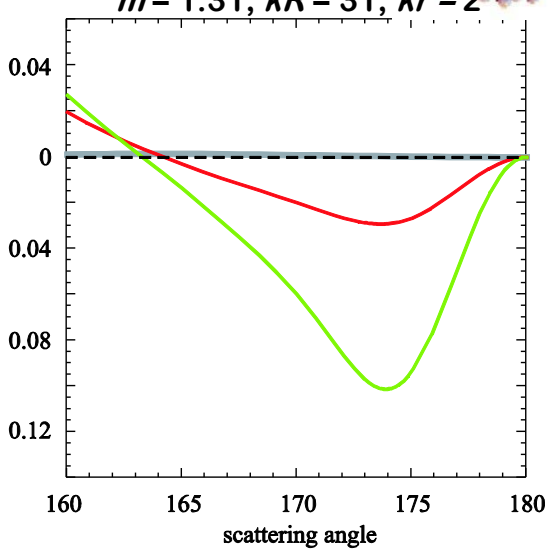

The BOE and POE can be accurately reproduced by a direct solution of the macroscopic Maxwell equations for a realistic model of the scattering medium ***(Mackowski & Mishchenko 2011)*****.**

No other theory of electromagnetic scattering has been demonstrated to get the BOE and POE simultaneously. Therefore, both opposition effects can be attributed, at least qualitatively, to coherent backscattering of sunlight by planetary surfaces composed of regolith particles with sizes comparable to or smaller than the wavelength ***(Mishchenko et al. 2011)*****.**

For more details see

Open-access publications

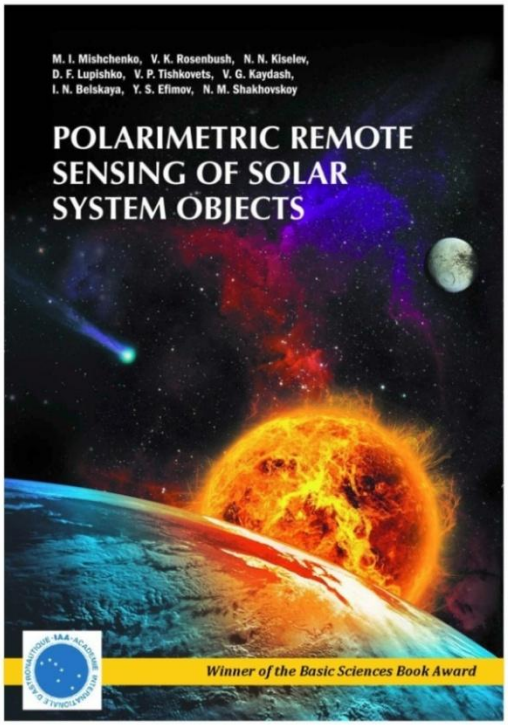

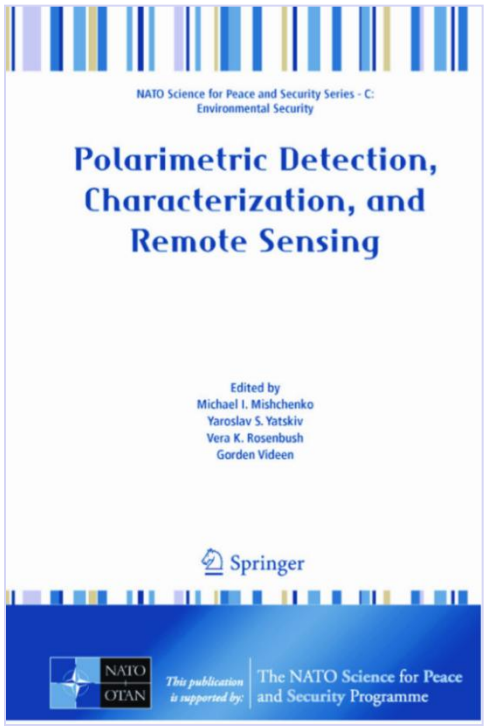

Thank You for attention!

Acknowledgments

- COST Action MP 1104 for travel funding to attend this Meeting
- my colleagues: N. Kiselev, S. Zaitsev, K. Antoniuk, S. Kolesnikov, V. Afanasiev, M. Mishchenko

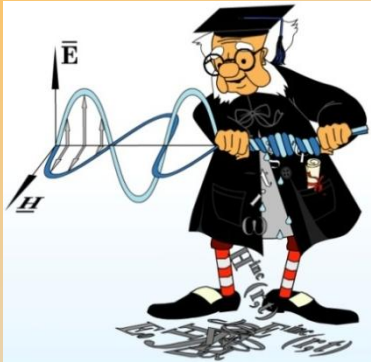

Urgent tasks and perspectives

A more detailed quantitative analysis of the observational data in terms of specific physical parameters of the regolith layer is hardly possible at this time given the limited observational dataset, the constrained theoretical ability to compute all photometric and polarimetric characteristics of the opposition phenomena for realistic polydisperse particle models, and the extreme morphological complexity and heterogeneity of the surfaces of the ASSBs.

Model ≠ Observations

Polarimetric and photometric observations of objects at different distances from the Sun in a broad spectral range, including UV and IR.

Inclusion in the space experiments measuring the polarization in a wide range of phase angles and wavelengths.

Improving remote sensing retrievals.

Application of theoretical models for interpretation of data.